

CHAPTER 2

FASTKD2 Nonsense Mutation in an Infantile Mitochondrial Encephalomyopathy Associated with Cytochrome C Oxidase Deficiency

Daniele Ghezzi,¹ Ann Saada,² Pio D'Adamo,³ Erika Fernandez-Vizarra,¹ Paolo Gasparini,³ Valeria Tiranti,¹ Orly Elpeleg,² and Massimo Zeviani¹

¹Division of Molecular Neurogenetics, Foundation IRCCS Neurological Institute "C. Besta," 20126 Milan, Italy

²Metabolic Disease Unit, Hadassah-Hebrew University Medical Center, 91120 Jerusalem, Israel

³Division of Medical Genetics, IRCCS Burlo Garofolo - University of Trieste, 34137 Trieste, Italy

The American Journal of Human Genetics 83, 1–9, September 12, 2008

Abstract

In two siblings we found a mitochondrial encephalomyopathy, characterized by developmental delay, hemiplegia, convulsions, asymmetrical brain atrophy, and low cytochrome c oxidase (COX) activity in skeletal muscle. The disease locus was identified on chromosome 2 by homozygosity mapping; candidate genes were prioritized for their known or predicted mitochondrial localization and then sequenced in probands and controls. A homozygous nonsense mutation in the *KIAA0971* gene segregated with the disease in the proband family. The corresponding protein is known as fas activated serine-threonine kinase domain 2, FASTKD2. Confocal immunofluorescence colocalized a tagged recombinant FASTKD2 protein with mitochondrial markers, and membrane-potential-dependent in vitro mitochondrial import was demonstrated in isolated mitochondria. In staurosporine-induced-apoptosis experiments, decreased nuclear fragmentation was detected in treated mutant versus control fibroblasts. In conclusion, we found a loss-of-function mutation in a gene segregating with a peculiar mitochondrial encephalomyopathy associated with COX deficiency in skeletal muscle. The corresponding protein is localized in the mitochondrial inner compartment. Preliminary data indicate that FASTKD2 plays a role in mitochondrial apoptosis.

Main Text

Mitochondrial disorders are clinical phenotypes associated with abnormalities of the terminal component of aerobic energy metabolism, i.e., oxidative phosphorylation (OXPHOS), a complex

pathway linking cellular respiration to adenosine triphosphate (ATP) synthesis. OXPHOS is carried out in the inner mitochondrial membrane by the mitochondrial respiratory chain (MRC). The MRC is composed of a series of multiheteromeric enzymes resulting from a dual genetic contribution, i.e., the nuclear and the mitochondrial genomes. Whereas the 13 MRC proteins encoded by mtDNA are all essential for OXPHOS, they make up only a tiny fraction of the total number of proteins involved in a functional MRC, most of which are in fact nucleus encoded and imported into mitochondria. As a consequence, mitochondrial disease can be due to mutations in either mtDNA or nuclear DNA genes functionally related to MRC and OXPHOS.¹ In fact, a huge number of pathogenic mutations of mtDNA have been building up in the last two decades, in association with a wide spectrum of clinical presentations. Albeit at a lesser rate, substantial progress has also been made in the characterization of nuclear OXPHOS-related genes responsible for mitochondrial syndromes.²

In addition to approximately 80 MRC structural subunits, OXPHOS nuclear genes encode a remarkable number of factors that control the formation, turnover, and activity of MRC, including mtDNA biogenesis and expression, and their adaptation to tissue- and development-specific needs.³⁻⁵ The size of the mitochondrial proteome is not precisely known, but the most recent studies have set it up to more than 1400 entries.^{6,7} Each of these genes and proteins may be considered as a candidate for disease. Therefore, it is not surprising that in spite of the tremendous expansion of scientific and medical knowledge in the field, the genetic etiology of many

mitochondrial clinical syndromes still remains elusive, the mechanisms leading to disease are poorly understood, and the very function of several factors involved in mitochondrial disorders is not, or is at best partially, known. Approximately 60% of biochemically defined OXPHOS disorders still fail to get diagnosed at the molecular level. To identify additional nuclear genes that cause mitochondrial disease phenotypes, we have embarked on a systematic, genome-wide linkage-analysis project based on homozygosity mapping of consanguineous multiplex families characterized by mitochondrial recessive traits.

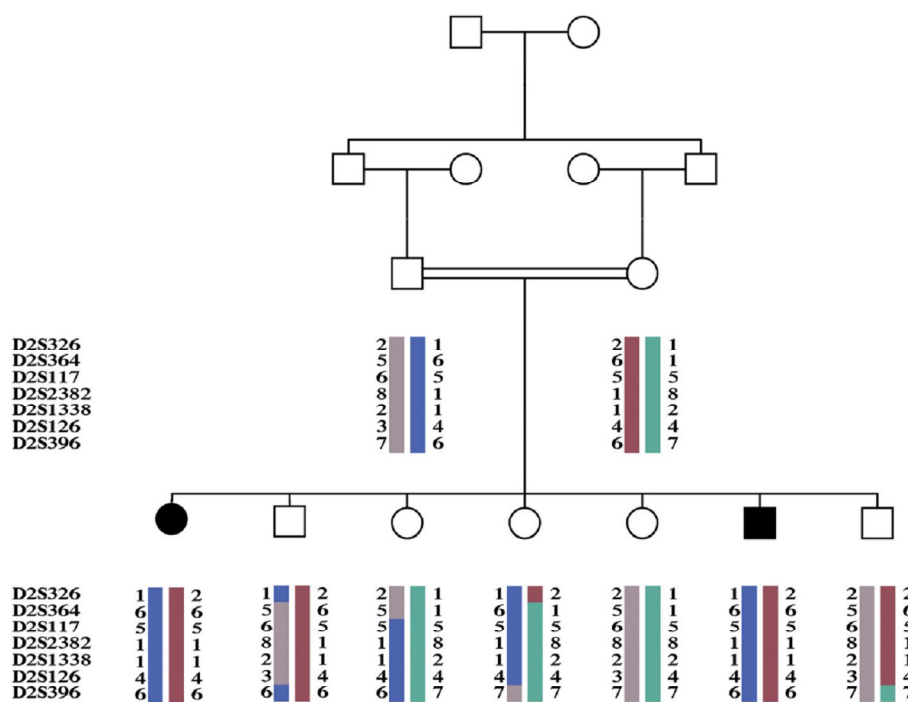


Figure 1. Pedigree and Haplotypes

Filled symbols indicate affected individuals. Each haplotype is indicated by a distinct color.

The family reported in this paper (Fig.1) is composed of first-cousin parents of Bedouin origin, with an offspring of seven siblings, two of whom are affected by a peculiar, early-onset encephalomyopathy.

Patient II-1, a female, was born at term after an uneventful pregnancy by caesarean section due to non-progression of labor. Birth weight was 3800 grams. Bilateral congenital hip dislocation was managed by abduction splinting. Marked irritability and inconsolable cry were noted since birth. Nonetheless, social and motor development was reported as normal until 7 months of age. At that time, she suffered from febrile illness and developed refractory generalized tonic-clonic convulsions. Because atypical pneumonia was suspected, she was treated with oral erythromycin. Brain MRI examination disclosed generalized symmetric atrophy (Fig.2A). In the following years, her epileptic disease persisted, the psychomotor development was markedly delayed, and left side hemiplegia ensued, with facial-nerve involvement. Brain CT scan performed at 5 yr of age revealed severe atrophic changes on the right hemisphere (Fig.2B). Because of fixed contractures, the hip and ankle tendons were surgically released at 7 yr of age. Echocardiography, abdominal ultrasound, blood count, and liver and renal functions were repeatedly normal and plasma lactate was mildly increased (2.4–3.2 mM in different samples; normal values [n.v.] < 1.8 mM). At 14 yr she obeyed simple commands in two languages, could recognize colours, and had a 20 word vocabulary. She could sit herself up and move herself relatively smoothly along the floor while sitting, but was never able to stand or walk. Her hearing was intact but the eyesight was impaired because of bilateral optic atrophy. She had left spastic hemiparesis; on the right

side the muscle tone was decreased with reduced strength (3/5). Myoclonic and gelastic seizures were partly controlled by carbamazepine, valproate, and clonazepam. The EEG revealed bilateral epileptic activity, which was more prominent over the left hemisphere. Biochemical assays were first performed in isolated mitochondria at Hadassah-Hebrew University Medical Center in Jerusalem, Israel. As shown in Table 1, the specific activity of cytochrome c oxidase (COX) was reduced to 21% of the control mean (3.1 nmoles/min/mg versus a control mean of 14.8 ± 3.6). The activities of the other MRC complexes, as well as that of the pyruvate dehydrogenase complex (PDHc), were within the control range. The respiratory-chain activities were measured 2 yr later in the muscle homogenate by a second laboratory, at the Istituto Neurologico “Carlo Besta” in Milan, Italy. Again, the activity of COX, normalized to that of citrate synthase (CS), was severely reduced, to 14% of the control mean, while the activities of complex II and III were in the lower limit of the normal or just below it (Table S1 available online). The activity of complex I could not be measured because of the scarcity of the material. In spite of the isolated COX defect detected in muscle homogenate, no gross abnormality of COX and succinate dehydrogenase (SDH) histochemical reactions were reported in muscle, and the trichrome Gomori stain was normal. The activities of all MRC complexes were normal in cultured skin fibroblasts (Table S1).

Patient II-6, the 6th child of the couple, was born at term, with a birth weight of 4150 gr. His early development was uneventful, and at 10 months he could sit himself up and crawl freely. After a febrile

gastroenteritis at 1 yr of age, the patient experienced subacute neurological deterioration with muscle hypotonia and extrapyramidal movements, mainly on the left limbs. Brain MRI disclosed increased signal intensities on the left nucleus caudatus, globus pallidus, and crus cerebri. The lateral ventricles and the basal cisternae were of normal size (Fig.2C). A convulsive disorder, first noted at around one year, became refractory to treatment at the third year of life. The patient went into prolonged periods of *status epilepticus*; the EEG disclosed flattening of activity over the right hemisphere and triphasic peaked waves over the left hemisphere. A brain CT scan at 30 months revealed generalized and white-matter atrophy, more pronounced on the left basal ganglia, with bilateral dilatation of the ventricles and basal cisternae (Fig.2D). At four years, he was bed-ridden with neither communication nor any voluntary activity. There was bilateral optic atrophy and strabismus. His general muscle tone was decreased with hyperreflexia and dystonic posturing. The gag reflex was weak and he was fed via gastrostome. He had two episodes of deep-vein thrombosis at sites of central-line catheters, but blood coagulation screen was negative. Echocardiography, abdominal ultrasound, blood count, blood gases, liver and renal function tests, urinary organic acids, plasma very-long-chain fatty acids, plasma lactate, and amino acid levels were normal. CSF lactate was increased to 3.8 mM (n.v. < 1.8 mM), and the activity of COX in his lymphocytes was reported as markedly decreased. No other biological material is available for this patient. The parents gave informed consent to a biochemical and genetic screening according to the Ethical Committee of Hadassah University Hospital, Jerusalem, Israel. Blood samples were collected

from parents and all seven siblings of the family; DNA was extracted by standard methods. However, 2 yr ago we lost contact with the family; therefore, we are currently unable to give an updated follow-up of the probands.

Table 1. Biochemical Assays on Pt II-1 Muscle Mitochondria

Enzyme	Specific	Control		
	Activity	Pt II-1	Mean \pm SD	%
Citrate Synthase	mmol/min/mg	1.4	2.12 \pm 0.37	66
Succinate-ubiquinone reductase	nmol/min/ng	56	77 \pm 15	73
Succinate dehydrogenase	nmol/min/ng	206	327 \pm 52	63
NADH-ferricyanide reductase	mmol/min/mg	2.7	4.65 \pm 1.02	58
NADH-cyt. c oxidoreductase	nmol/min/mg	445	586 \pm 186	76
Succinate-cyt. c oxidoreductase	nmol/min/mg	251	333 \pm 100	75
Cytochrome c oxidase	mmol/min/mg	3.1	14.8 \pm 3.6	21
Mg ATPase with DNP	pmol/min/mg	888	721 \pm 203	123
PDHc	nmol/min/mg	81	80 \pm 24	101

Depletion of mtDNA and mtDNA large-scale rearrangements were ruled out in skeletal muscle of patient II-1 by real-time PCR⁸ and long-PCR analysis,⁹ respectively. Pathogenic mtDNA point mutations were also excluded by sequence analysis of the entire mtDNA molecule¹⁰ from skeletal muscle of the same patient.

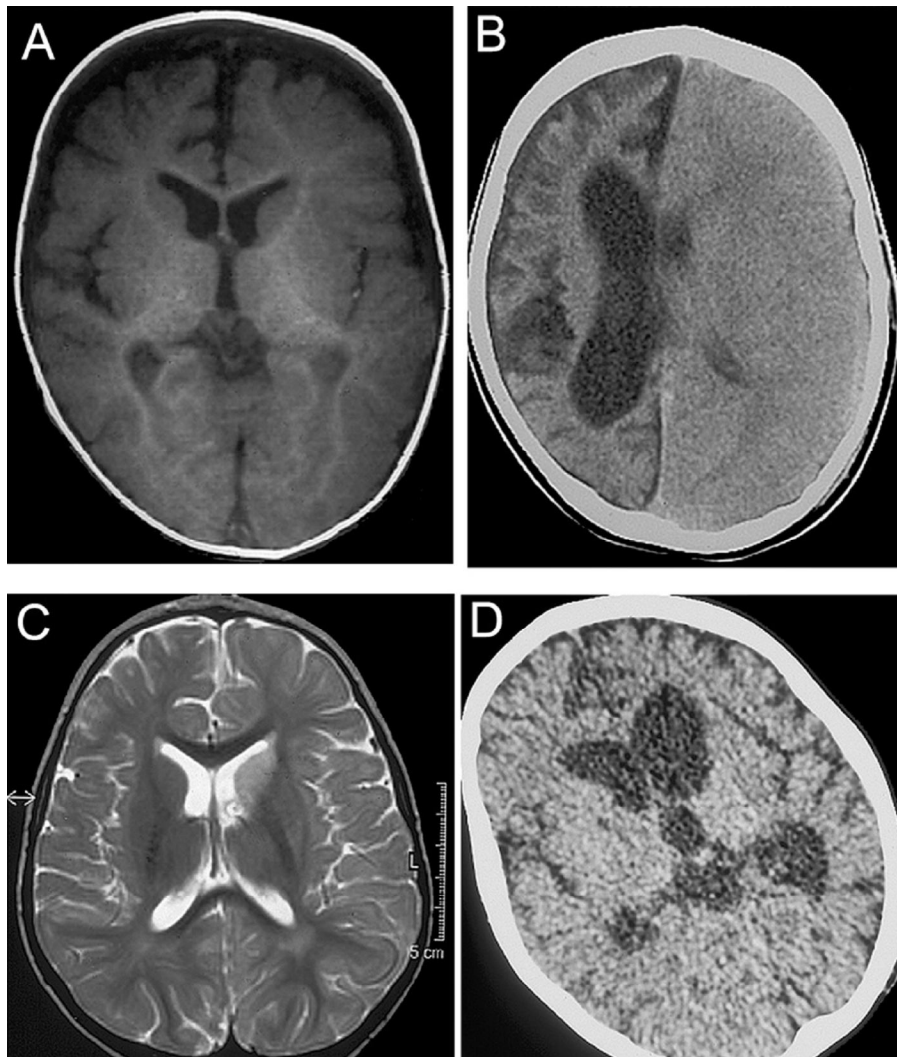


Figure 2. Brain Imaging

(A) Magnetic resonance imaging (MRI) T1-weighted sequence on a transverse section of supratentorial brain of patient II-1 at disease onset (7 months of age). (B) Computerized tomography (CT) scan of the brain in patient II-1 at 5 yr. (C) MRI T2-weighted sequence on a transverse section of supratentorial brain in patient II-6 at disease onset (1 yr of age). (D) CT scan of the same brain section in patient II-1 at 30 months.

A nuclear-genome-wide search was performed with the ABI PRISM Linkage Mapping Set v.2.5 (Perkin Elmer, USA), characterized by

over 375 markers that define a 10 cM resolution human index map. PCR reactions with fluorescently labeled primers were run under the conditions suggested by the supplier. An aliquot of each PCR reaction was run on an ABI PRISM 3100 DNA sequencer, and results were processed by GENEMAPPER software. Statistical analysis was performed on the basis of an autosomal-recessive disease with complete penetrance. Multipoint parametric linkage analysis was performed with SIMWALK2 2.91.¹¹ The linkage analysis in the family gave a pairwise lodmax score of 2.428 on D2S1338. A region with a LOD score of ~2 is located between recombinant markers D2S326 and D2S396 on chromosome 2q31-q36 (Figure S1, available online). No other genomic region gave positive lod scores by linkage analysis, suggesting that the 2q31-q36 contained the responsible gene.

Haplotype reconstruction revealed a homozygous condition caused by identity-by-descent alleles in the affected individuals (Fig.1). Because of their biochemical and clinical features, we assumed that the responsible protein was likely to be involved in mitochondrial metabolism and be targeted to mitochondria.

The D2S326-D2S396 interval contains 382 gene entries, some of which encode proteins that are known to target to mitochondria. Other genes within this interval encode unknown polypeptides that score high when analyzed with dedicated prediction softwares for mitochondrial targeting, including MitoProt, TargetP, and PSORT-II. Sequencing of coding regions of 14 such genes (Table S2) failed to reveal disease-segregating mutations, with the exception of a homozygous missense mutation in the gene encoding BCS1L, an

assembly factor of MRC complex III (CIII).¹² The mutation predicts a p.D210N amino acid change in a conserved region of the BCS1L protein. However, the presence of an isolated defect of complex IV (CIV) rather than CIII in the muscle of patient II-1, the absence of an assembly defect of CIII in either muscle or fibroblasts (Figures S2), and the detection of the p.D210N mutation in one out of 240 chromosomes from Italian control samples cast doubts about its pathogenic role. We then sequenced the exons and the intron-exon junctions of an anonymous gene entry (*KIAA0971*; primer sequences are available upon request) encoding a protein with a high score for mitochondrial targeting. The *KIAA0971* cDNA (NM_014929) corresponds to a gene spanning 27 kb and organized in 12 exons. The open reading frame (ORF) of *KIAA0971* predicts an amino acid sequence that contains a Fas-activated serine-threonine (FAST) kinase domain (NP_055744) and is therefore known as FASTKD2, for FAST kinase domain protein 2 (MIM 606965). However, the human FASTKD2 N terminus contains two potential translation-initiation methionine residues, at position +1 and +17 (M1, M17); both M1 and the sequence between M1 and K16 are absent in all of the nonhuman species in which FASTKD2 is present, i.e., mammals and birds, including the closest living human relatives, e.g., *Pan troglodytes* and *Pongo pygmaeus*, whereas M17 and the rest of the protein sequence are both conserved (Fig.S3A). For instance, in both *Pan troglodytes* and *Pongo pygmaeus*, the potential predicted sequence corresponding to M1–M17 is identical to the human sequence, except that isoleucine is present at the apparent amino acid position 1 instead of methionine, whereas the methionine at position 17 is conserved (Fig.S3B). Taken

together, these observations strongly suggest that in humans as in other species, the “true” FASTKD2 protein starts from M17 rather than from M1. Moreover, when mitochondrial-targeting prediction softwares are used, the sequence starting at the alleged M1 residue scores relatively high for mitochondrial targeting, but that from M17 scores much higher (Mitoprot 72% versus 91%; TargetP 43% versus 76%). Therefore, we considered the sequence starting from M17 as the bona fide physiological human *KIAA0971*-encoding protein; it is hereafter referred to as FASTKD2 and consists of 694 amino acid residues, instead of the potentially translatable 710 residues. According to the nucleotide numeration of NM_014929, and considering the ATG encoding M17 as the translation initiation codon, we found a homozygous c.1246C→T nucleotide transition in both patients, whereas the two parents were heterozygous (Fig.3A). The c.1246C→T change determines the conversion of a CGA triplet, encoding R416, into a TGA termination codon. This is by definition a deleterious change (R416X) predicting the synthesis of a prematurely truncated protein, missing the 278/694 C-terminal amino acid residues (Fig.3B). The mutation was absent in 240 control alleles. The missing portion of the mutant *KIAA0971* protein sequence contains two predicted transmembrane domains (403–421 and 482–500 amino acid residues), as well as the FAST kinase domain. Whereas the function of FASTKD2 is presently unknown, previous work showed FAST to be anchored to the outer face of the outer mitochondrial membrane, from where it plays an inhibitory role in the activation of the Fas-dependent apoptotic cascade.¹³

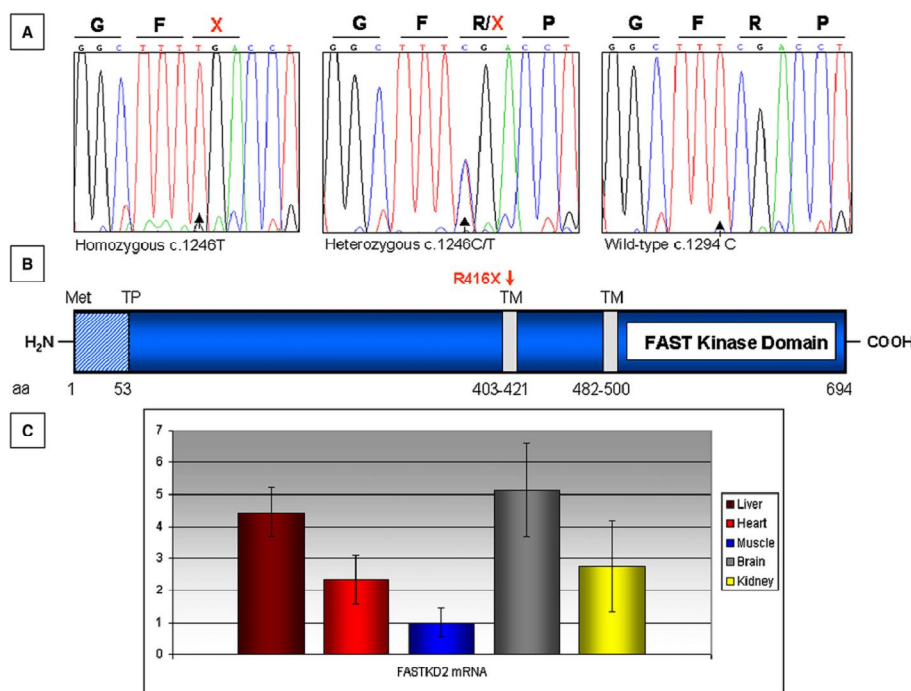


Figure 3. FASTKD2 Features

(A) Sequence analysis of exon 7 of KIAA0971 showing the c.1246C/T change in patient II-1 (homozygous T), her father (heterozygous C/T), and a control (homozygous C). (B) Schematic structure of FASTKD2 protein. TP indicates a predicted cleavage site; TM indicates two putative transmembrane domains. A red arrow indicates the position of the R416X mutation. (C) Quantitative real-time PCR of FASTKD2 mRNA relative to GAPDH mRNA in different mouse tissues. The relative amount of FASTKD2/GAPDH mRNA in muscle was taken as reference. Errors bars indicate the standard deviation (\pm SD).

In order to establish experimentally the subcellular localization of FASTKD2, a sequence encoding a hemagglutinin (HA) tag of the influenza virus was added in frame at the 3' end of the KIAA0971 ORF encoding FASTKD2, and the modified cDNA was inserted into pCDNA3.2 (Invitrogen), a mammalian expression vector. This construct was then transfected by electroporation in COS7 cells and HeLa cells. After 24 hr, cells were incubated with a monoclonal anti-

HA and a polyclonal anti-mtSSB (mitochondrial single-strand-DNA binding protein) antibody. Immunofluorescence images were acquired with a confocal microscope (Biorad). As shown in Figure 4, the FASTKD2^{HA}-specific immunofluorescence pattern obtained with the anti-HA antibody coincided with that of mtSSB, a mitochondrion-specific protein. This result demonstrates that FASTKD2^{HA} targets to mitochondria. Mitochondria are double-membrane organelles; therefore, mitochondrial proteins can be localized in the outer mitochondrial membrane (OMM), in the mitochondrial intermembrane (MIM) space, or in the inner mitochondrial compartment (IMC), consisting of the inner mitochondrial membrane (IMM) and the mitochondrial matrix (MM). Translocation into the IMC is an energy-dependent process requiring both ATP and a mitochondrial membrane potential ($\Delta\Psi$).¹⁴ For demonstration of active mitochondrial import into the IMC, [³⁵S]-radiolabeled in vitro-translated FASTKD2, obtained with the TNT Quick Coupled Transcription/Translation Systems (Promega), was incubated for 45 min at 37°C with freshly prepared HeLa-cell mitochondria energized by the addition of ATP in the presence or absence of 20 μ M valinomycin.¹⁵ After incubation, some samples were treated with proteinase K (PK), with or without the previous addition of PMSF, an inhibitor of PK, and/or Triton X-100, a detergent that disrupts membranes. All samples were loaded into SDS-PAGE; after fixation in 10% acetic acid and 25% isopropanol, the gel was washed for 20 min in Amplify reagent (Amersham) and layered onto a phosphorimaging screen (Biorad). After overnight exposure,

autoradiography was carried out in a Molecular Imager apparatus (Biorad).

Upon exposure to freshly prepared energized mitochondria, two radiolabeled bands were visualized (Fig.4D), a larger band corresponding to the full-length in vitro-translated FASTKD2 and a shorter one corresponding to a mature protein species lacking an N-terminal mitochondrial target sequence. A potential cleavage site of the 79 kDa FASTKD2 precursor protein by the mitochondrial matrix protease (MMP) is present between M52 and Q53 and predicts the mature imported protein from the FASTKD2 precursor to be composed of 642 amino acid residues for a MW of approximately 73 kDa. The two bands shown in lane 2 correspond nicely to the size of either FASTKD2 protein species. Treatment with PK determined the complete digestion of the upper band in intact mitochondria, whereas a substantial amount of the lower band was left intact, as expected to occur for a protein species imported into, and protected by, the IMC. This digestion is specific and can be blocked by the addition of PMSF. After treatment of the mitochondrial membranes with Triton X-100, exposure to PK determined the complete digestion of both protein species, again indicating that the shorter polypeptide was located inside the IMC of the organelle. As reported for other mitochondrial IMC proteins, the import process was dependent on the presence of a mitochondrial proton-motive force ($\Delta\Psi$), because it was blocked by treatment of the mitochondrial suspension with valinomycin, an ionophore drug that dissipates $\Delta\Psi$. These results demonstrate that FASTKD2 is indeed imported into the IMC through the $\Delta\Psi$ -dependent TOM-TIM import machinery, which targets proteins to

either the IMM or the MM.¹⁶ The presence of two predicted transmembrane domains suggests that FASTKD2 is anchored to the IMM, and the full protection from PK digestion indicates that it may project toward the IMC.

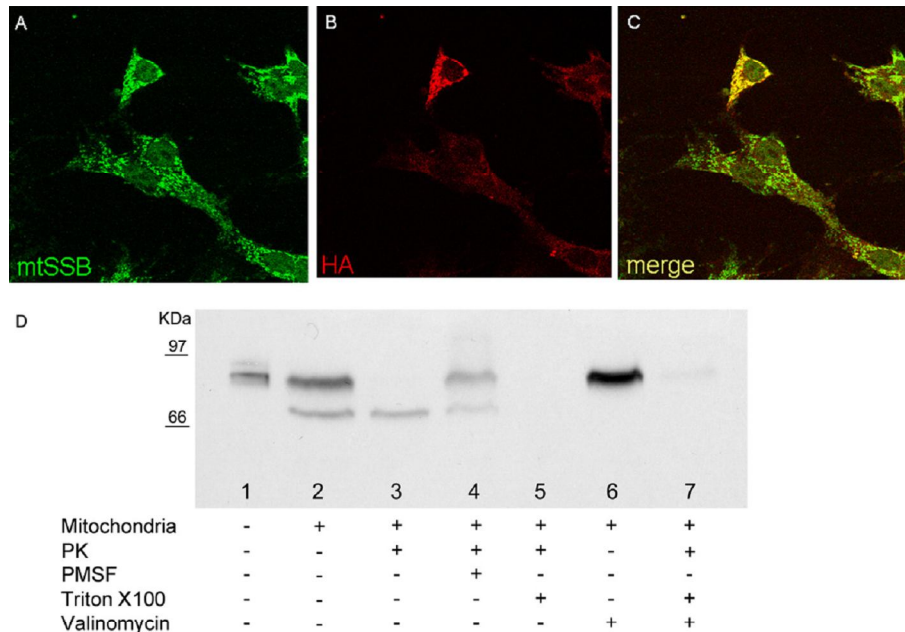


Figure 4. Immunofluorescence and In Vitro Import Assay

(A) Immunofluorescence specific to mtSSB.

(B) Immunofluorescence specific to FASTKD2HA.

(C) Merge. All images were taken in COS7 cells 24 hr after FASTKD2HA transfection.

(D) Import assay on isolated HeLa cell mitochondria. Lane 1, in vitro-translated FASTKD2; lane 2, FASTKD2 + mitochondria; lane 3 FASTKD2 + mitochondria + PK; lane 4, FASTKD2 + mitochondria + PK + PMSF; lane 5, FASTKD2 + mitochondria FASTKD2 + PK + Triton X-100; lane 6, FASTKD2 + mitochondria + valinomycin; and lane 7, FASTKD2 + mitochondria + valinomycin + PK.

Electronic data from arrays available in public databases (Genecards) shows that FASTKD2 is ubiquitously expressed. To measure FASTKD2 gene expression experimentally, we created specific primers for the mouse ortholog (NM_172422). Then we extracted

RNA from different mouse tissues, and first-strand cDNA was synthesized by standard methods. We analyzed by real-time PCR the abundance of the FASTKD2 transcript, normalized via the GAPDH transcript as reference. FASTKD2 transcript was expressed ubiquitously, but in variable amounts from tissue to tissue, with skeletal muscle < heart \leq kidney < liver \leq brain (Fig.3C).

Because nuclear genes coding for assembly factors of COX, such as SURF-1, are known to cause CIV deficiency, a role for FASTKD2 in COX assembly was evaluated by blue-native gel electrophoresis (BNGE)-western-blot analysis.¹⁷ However, we failed to demonstrate abnormality in the assembly status and abundance of COX by using an anti-COX1 antibody complex, in muscle of patient II-1 (Figure S2). Therefore, whether the COX defect is a direct and specific consequence of, or is rather part of a more general mitochondrial dysfunction induced by, the abolishment of FASTKD2 remains an open issue for future investigation.

The presence of a FAST domain in FASTKD2 and the involvement of FAST in the apoptotic process prompted us to evaluate nuclear fragmentation, taken as an index of apoptotic response,¹⁸ in mutant versus control fibroblasts incubated with 1 mM staurosporine for 3 hr (Fig.5A). Staurosporine, a potent protein kinase C inhibitor, is known to induce apoptosis through a mitochondria-mediated pathway¹⁹ and to cause oxidative stress through mitochondrion-generated ROS in several cells.²⁰ As shown in Figure 5B, the percentage of fragmented nuclei in mutant cells was significantly lower than that of control cells (Chi-square value = 0.003).

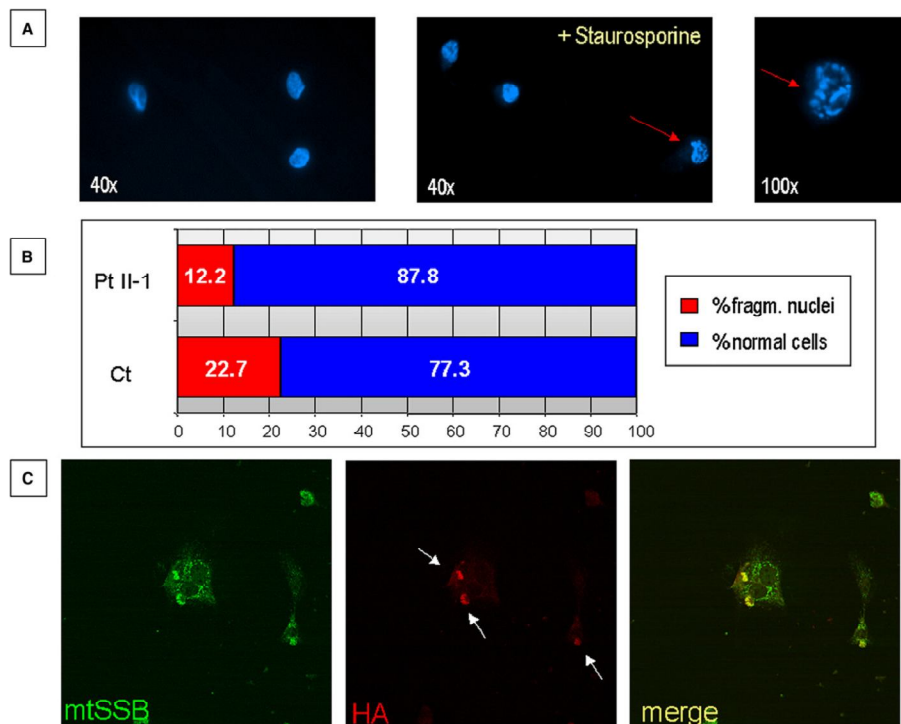


Figure 5. Staurosporine-Induced Apoptosis

(A) Hoechst staining of fibroblasts before and after staurosporine treatment. Red arrows indicate cells with fragmented nucleus.
 (B) Quantification of cells with fragmented nucleus in control (Ct) and patient (Pt II-1) fibroblasts.
 (C) Immunofluorescence images of COS7 cells 48 hr after FASTKD2^{HA} transfection.

This result suggests a specific role of FASTKD2 in the regulation of mitochondrial apoptosis, because it does not seem to depend upon the activity of the respiratory-chain complexes that were all in the normal range in mutant fibroblasts. In support of this hypothesis stands the observation that overexpression of recombinant FASTKD2^{HA} in HeLa or COS7 cells consistently led to shrinkage of the cell body, followed by nuclear fragmentation and eventually apoptotic death (Fig.5C). As a consequence, we were unable to generate stably overexpressing

FASTKD2^{HA} cell lines. Whether this drastic effect is due to a specific function of FASTKD2, or to a generic toxic effect due to damage of the inner mitochondrial membrane, remains to be elucidated.

The clinical and MRI findings of the FASTKD2-associated disease are rather unusual for mitochondrial disorders. Combination of hemiplegia and epilepsy may be reminiscent of mitochondrial encephalomyopathy with lactic acidosis and stroke-like episodes (MELAS, MIM #540000),²¹ but other features were missing, including RRF and lactic acidosis. Other signs were peculiar of this syndrome and resembled some key features of Rasmussen's encephalopathy, an allegedly immunological condition characterized, like our probands, by infantile onset, intractable epilepsy, emispheric atrophy with dilatation of the ipsilateral ventricle system, and hemiparesis with a slowly progressive, relentless course.²² However, we failed to identify mutations in the *KIAA0971* sequence in five consecutive patients with Rasmussen's encephalopathy, suggesting that the *KIAA0971*-associated syndrome is a genetic condition that phenocopies but does not account for sporadic Rasmussen's encephalopathy.

In conclusion, we found a previously unreported gene mutated in a peculiar mitochondrial COX-defective encephalomyopathy. We demonstrated that the responsible protein, FASTKD2, is localized in the IMC, where it may play a still-unknown role in apoptosis. Although FASTKD2 is not directly involved in COX assembly, its ablation is indeed associated with COX deficiency in skeletal muscle. The elucidation of the function of FASTKD2 is made difficult by the likely rarity of the clinical condition linked to its disruption (to our

knowledge, this is the first and so far only family with a FASTKD2 mutation) and by the difficulty to establish cell lines stably expressing recombinant FASTKD2^{HA}. In addition, FASTKD2 seems to be present only in mammals and birds, whereas no orthologs can be found in other animals, plants, and lower eukaryotes. This prevents the possibility to create models in user-friendly organisms such as yeast, worm, or fly. The restriction of FASTKD2 to relatively recent classes of animals, notably those endowed with homeothermy, may suggest a role for FASTKD2 in the finely-tuned regulation of heat production by mitochondria. The use of siRNA in cell culture, and the creation of a murine knockout model for the FASTKD2 gene, which is under way in our laboratory, will help clarify the function of this new, elusive component of the IMC and give a mechanistic interpretation to the mitochondrial syndrome affecting humans.

Web Resources

The URLs for data presented herein are as follows:

- ClustalW, <http://www.ebi.ac.uk/Tools/clustalw/index.html>
- Ensembl, <http://www.ensembl.org>
- GeneCards, <http://www.genecards.org/index.shtml>
- Mitoprot, ihg2.helmholtz-muenchen.de/ihg/mitoprot.html
- NCBI database, <http://www.ncbi.nlm.nih.gov>
- Online Mendelian Inheritance in Man (OMIM), <http://www.ncbi.nlm.nih.gov/Omim/>
- Psort II, <http://psort.ims.u-tokyo.ac.jp/form2.html>
- TargetP, <http://www.cbs.dtu.dk/services/TargetP>
- TMpred, http://www.ch.embnet.org/software/TMPRED_form.html

Supplemental Data

Supplemental Data include two tables and three figures and can be found with this article online at <http://www.ajhg.org/>

Supplemental table I: Respiratory chain activities of muscle homogenate and fibroblasts of PtII-1 normalized to the activity of citrate synthase (CS).

Pt II-1 muscle*	enzyme/CS	Control mean (\pmSD)	%
Succinate-ubiquinone reductase	8.4	21.5 \pm 6.5	39
Succinate dehydrogenase	9.7	14 \pm 3.3	69
NADH-ubiquinone reductase	n.d.	18.5 \pm 5.5	-
DBH2cytochrome reductase	42	127.5 \pm 39.5	33
Cytochrome c oxidase	23	170 \pm 50	14
Mg ATPase	273	155 \pm 66	176
Pt II-1 fibroblasts**			
Succinate-ubiquinone reductase	14.2	13.5 \pm 4.9	105
Succinate dehydrogenase	9.3	10.4 \pm 3.9	89
NADH-ubiquinone reductase	26.4	18.4 \pm 7.7	143
DBH2cytochrome reductase	105	108.3 \pm 21.8	97
Cytochrome c oxidase	129	124.6 \pm 37,6	104
Mg ATPase	102	89.2 \pm 23.5	112

*Citrate synthase (CS) specific activity in muscle: 100 nmol/min/mg (normal control 145 \pm 65) **CS specific activity in fibroblasts: 156 nmol/min/mg (normal control 150 \pm 50). n.d.= not determined

Supplemental table II. List of the genes in the disease locus analyzed by sequencing

Symbol	Official full name	Protein accession number
MT-ABC3	Mitochondrial ATP-binding Cassette 3	NP_005680
MARS	Mitochondrial methionyl-tRNA synthetase 2	NP_004981
MRPL44	Mitochondrial ribosomal protein L44	NP_075066
MTX2	Metaxin 2	NP_001006636
HSPD1	Heat shock 60kDa protein 1 (chaperonin)	NP_955472
HSPE1	Heat shock 10kDa protein 1 (chaperonin 10)	NP_002148
BCS1L	BCS1-like (yeast)	NP_004319
GLS	Glutaminase	NP_055720
NIF3L1	NIF3 NGG1 interacting factor 3-like 1 (<i>S. pombe</i>)	NP_068596
ADAM23	ADAM metallopeptidase domain 23	NP_003803
PNKD	Paroxysmal nonkinesigenic dyskinesia	NP_056303
OSGEPL1	O-sialoglycoprotein endopeptidase-like 1	NP_071748
C2orf47	Chromosome 2 open reading frame 47	NP_078796
COQ10B	Coenzyme Q10 homolog B (<i>S. cerevisiae</i>)	NP_079423
FASTKD2	FAST kinase domain 2	NP_055744

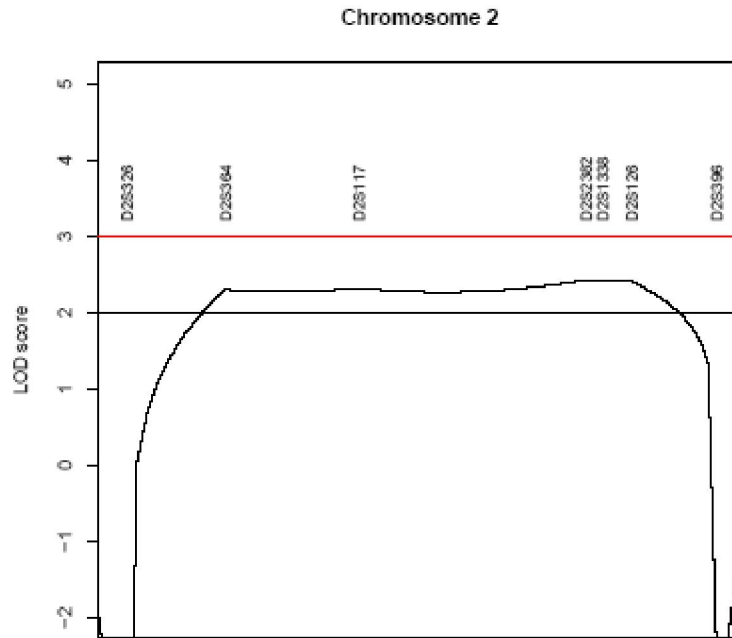


Figure S1. Multipoint linkage analysis

The graph represents the region between markers D2S326 and D2S396 with a location score ≥ 2 . A pairwise lodmax score of 2.428 was on D2S1338.

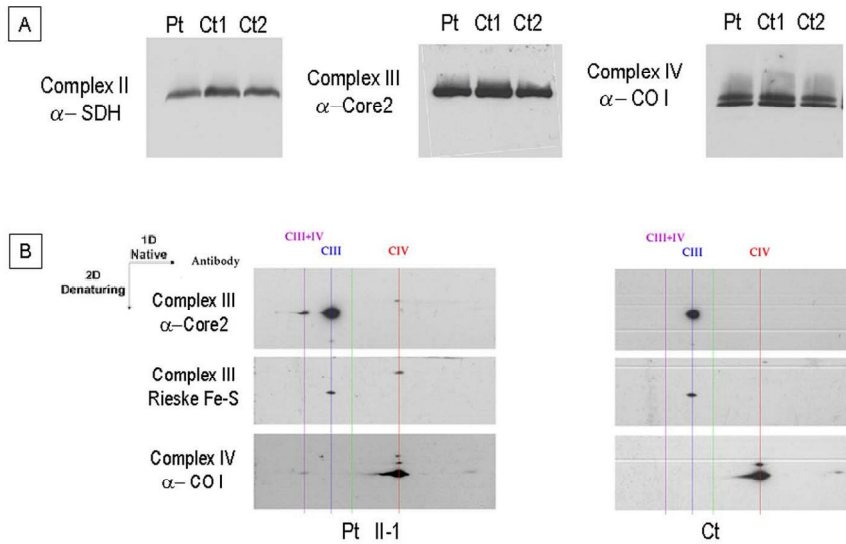


Figure S2. BNGE of patient and control muscle

Panel A. One-dimension BNGE of muscle homogenates from patient II-1 (Pt) and 2 controls (Ct1 and Ct2). An antibody against the SDH 30 kDa subunit was used to detect complex II; an antibody against Core2 was used for complex III; and an antibody against COX-I was used for complex IV.

Panel B. Second-dimension BNGE of patient II-1 (Pt) and control (Ct) muscle homogenates. Antibodies against Core2 and Rieske Fe-S protein were used to detect complex III; an antibody against COX-I was used for complex IV.

A)

```

Homo      MNNKAGSFFWNLRFSTLVSTSRMTMLCCLGLCKPKIVHSNWN---ILNPFHNRMQSTD 56
Pongo     MNNKAGSFFWNLRFSTLVPTSRMTMLRYRLGLCKPKIVHSNWN---ILNPFHNRMRSTD 56
Bos       MTNRAGSFLWNLRLQLSTLVPTGRVRLYPLAFCRPNIAYSNWNRR--NLLNTFGNKMHSS- 58
Mus       MNSKARSLLWTRIRRFSTLLPRSRLRIDPLGTCRPEVIHSKWNPRNHRNLNVFDEGLQPS- 59
Gallus    MGYLLNAVRY-LRR CSPVPRPSAPTSRHVVWTRHRDCLDNTNCRTLFLNAPFSLRGS- 58
*       . : . : * : * : . : . : . : . : . : . : *       * * * . . .

Homo      IIRYLFQDAFIFKSD-VGFQTKGISTLTALRIERLLYAKRFFDQSKQSLVPVDKSDDELK 115
Pongo     IIRYLFQDAFIFKSD-VGFQTKGISTLTARRIERLLYARRLFFDQSKQSLVPVDKSDDGLK 115
Bos       -TRYLFQDALIFKSEGDGCQTKGINTAVFTVVDKLLCPRRLSFDSKHFLVSVN---ELK 113
Mus       -VRYLFQDIFISKSVVDCIQTKGISHSVAFKPDRLLCPRRLSFDKHSFVSDGTDHDLK 118
Gallus    -LRFLSHKADAFVGVDEVQQEK-----SREAAVSEQAPQSSLE 95
* * : . * * : . : * . * :

Homo      KVNLNHEVSNEDVLTKETKPNRISSRKLSSECNSLSDVLDAPSKAPTFPSSNYFTAMWTI 175
Pongo     KVNLNHEVSNEDVLTKETKPNRISSRKLSSECNSLSDVLDAPSKAPTFPSSNYFTAMWTI 175
Bos       KS-FHQEASDEDVLTKRRKPALISSTKLSQECNSLSDVLDIFSKAPTFPSSNYFSAMWTI 172
Mus       KINFHHTSS-EDVFTKKVRPTPVNYKLAQECNSLSDVLDTFSKAPTFPSSNYFLAMWTI 177
Gallus    LEKLEGGDAQSFRVKAALDENEQFFNRLHTCACPSDVLDLASESAVSIKQFTNCLTITWKL 155
: . : . : * : . : . : . : * * * * * * * * * * * * : : * : * :

Homo      AKRLSDDQKRFKRLMFSHPAFNQLCEHMMREAKIMQYKYLFLSLHAIVKLGIPQNTILV 235
Pongo     AKRLSDDQKRFKRLMFSHPAFNQLCEHMMREAKIMQYKYLFLSLYSVMVKGIPQNTILV 235
Bos       AKRMSDDQKRFKRLMFSHPAFNQLCEHMMREAKIMYFGDLLFSLHAIVKLGIPQNTILV 232
Mus       AKRISDDQKRFKRLMFSHPAFNQLCEHMMREAKIMHYDHLFLSLHAIVKLGIPQNTILV 237
Gallus    LRSMSDDQRRYKRLVFEHPAFVRLCQQLLRDRMRTRGDLVFLSHAVNLVGPQNTILV 215
: : * : * : * : * : * : * : * : * : * : * : * : * : * : * : * : * : * :

Homo      QTLLRVTQERINECDEICLSVLSTVLEAMEPCKNVHVLRTGFRILVDQVWVKIEDVFTLQ 295
Pongo     QTLLRVTQERINECDETCLSVLSAVLEAMEPCKNVHVLQMGFRILVDQVWVKIEDVFTLQ 295
Bos       QTLLRVVQERINECDEKCLSVLSTILNTEPCKNVVLLAGLRMLVDEQVCKIKHVFTLQ 292
Mus       QTLLRTIQERINECDEKCLSVLSTALVSMPCMNVNALRAGLRILVDQVWVNIKHVFTLQ 297
Gallus    QTLLRVQCEKLNQLDNRCMSVLATTLAGMDEDKNVSALQAGLQLLVEQRLPSIRDFILQ 275
***** * : * : * : * : * : * : * : * : * : * : * : * : * : * : * :

Homo      VVMKCIQKDAPIALKRKLKEMKALRELDKRSVLNSQHMFEVLAAMNHRSLILLDECSKVV 355
Pongo     VVMKCIQKDAPIALKRKLKEMKALRELDKRSVLNSQHMFEVLAAMNHRSLILLDECSKVV 355
Bos       TVMRSIGKDAPIGLKRLKEMKALRELDKRSVLNSQHMFEVLAAMNHRSLILLDECSKRV 352
Mus       TVMKCIQKDAPIALKRKLKEMKALRELDKRSVLNSQHMFEVLAAMNHRSLILLDECSKVI 357
Gallus    NLMKCMGKDAPIVLLKRLKEMAVLREIDHLYPNHRVFLGLVAMNYCSIPVNLNCSKIKLQ 335
* : * : * : * : * : * : * : * : * : * : * : * : * : * : * : * : * : * :

Homo      DNIHGCPRLRIMINILQSKDLQYHNLDFKGLADYVAATFDIWKFRKVLFIILFENLGF 415
Pongo     DNIHGCPRLRIMINILQSKDLQYHNLDFKGLADYVAATFDIWKFRKVLFIILFENLGF 415
Bos       SNIHGCPFKILINILQSKDLQYINIDLKGLADYVATFDIWKFRKVLFIILFENLGF 412
Mus       DNVHGCPPFKILISILQSKDLRYQNEKLSIAEYVATFDIWKLVQVIFLLLFETLGF 417
Gallus    ENIHDAPYQWLLILILEACHSLQYRNILKLSAVADYVNSIVCLLDKQIILFLSAFETLGF 395
. * : * : * : * : * : * : * : * : * : * : * : * : * : * : * : * : * :

Homo      RVPGLMDLFMKRIVEDPESLNMKNILSLHTYSSLNHVYKQCNKEQFVEMASALTGYLH 475
Pongo     RVPGLMDLFMKRIVEDPESLNMKNILSLHTYSSLNHVYKQCNKEQFVEMASALTGYLH 475
Bos       RVPGLMDLFIKKADEPGFLNVKSLVGLLNVSLSLNHFYKQCT-HEFLEVMASALTGSLH 471
Mus       RPPGLMDKLMKVVQEPGSLNVKNIVSILHVYSSLNHVHVIHN-REFLEALASALTGCLH 476
Gallus    QPSELMGVLAEKVTEDESEFLDKSFLIVLRVYSRLNYPVPGQH-LLFYETLHSCNLKYLQ 454
* * * : : : . : . * : * : * : * : * : * : * : * : * : * : * : * :

Homo      TISSENLLDAVYSFCLMNYFPLAPFNQLLQKDIISELLTSDDMK--NAYKLHMLDTCCLK 533
Pongo     TISSENLLHAVYSFCLMNYFPLAPFNQLLQKDVISELLTSDDMK--NVYKLHMLDTCCLK 533
Bos       HISENLLNAVCSFCWMNCFPLALINQLLQKDIIDLLTSGDVER-NVHRLHVATCCLK 530
Mus       HISESLLNAVHSCFMNCFPLAPINQLIKENIINELLTSGDTEK-NIHKLHVNTCCLK 535
Gallus    QISNAELLKAVYSLCILGYLPHLALNQLLQKDSFEELMSGDLYKREKREMMHLHCVTCMEL 514
* * . * * * * : * : * : * : * : * : * : * : * : * : * : * : * : * : * :

Homo      DDTVYLRDIALSLPQLPRELPSSTNAKVAEVLSSLLGGEGHFSKDVHLPHNYHIDFEIR 593
Pongo     DDTVYLRDIALSLPQLPRELPPSHPNKVAEVLSTDRS-PHNFPAKAAVATNSTHIYFEIR 592
Bos       DDAPCHKDLDLVLPQLPPMTPCPQP--KVAAVLSDLLG-EGCFSQSVQLPHNYHIDFEIR 587
Mus       DESTY-KSVHILPLQLP--LSASQPNKLAEVLSSRLLEGEGRFSRNVPLPHNYHIDFEIR 592
Gallus    DSPSPMKPAFVPTEIFSSLVSVTLR--KAREALLELLGDENMFRQNVQLPYEYRIDFEIR 572
* . . : : . : . * * * * * * * * * * * * * * * * * * * * *

```

```

Homo      MDTNRNQVLPLSDVDTTSATDIQRVAVLCVSRSAAYCLGSSHPRGFLAMKMRHLNAMGFHV 653
Pongo    MDTNRNQVLPLSDVDTTSATDIQRVAVLCVSRSAAYCLGSSHPRGFLAMKMRHLNAMGFHV 652
Bos      MDANRSQVLPPSNVDVVTSTDIQRVAVLCVPSAYCLDSTHPKGYLAMKMRHLKIMGFHV 647
Mus      MDTNRNQVFPFSDVDASSATNMQRVAVLCVPSVYCLNSCHPRGLMAMKIRHLNVMGFHV 652
Gallus   MDSDTKKVLPITATDSYADRSVQRLAFLFVPPSAFCLGTTHPQGLAMKRRHLSKLGYHV 632
          **:: :*::: : * : : : **:* * * . * . : ** : ** * * : ** * : ** * * * : : : *

Homo      ILVNNWEMDKLEMEDAVTFLKTKIYSVEALPVAAVNVQSTQ 694
Pongo    ILVNNWEMDKLEMEDAVTFLKTKIYSVEALPVAAVNVQST- 692
Bos      ILVNNWEVEKLEMKDAVAFLKTKIYSPKALSSAD IHLQSTC 688
Mus      ILIHNWELKKLKMEDAVTFVRKKIYSDEVLP TADTTV--- 689
Gallus   IPVLNKKFQELTNEGAIEFLKGIYSENVSPFSEVNLCDNN 673
          * : * : . : * : . : * : : : * * * : . : . : :

```

B)

```

Homo      MLTTLKPPGVSVESKMNNKAGSFFWNLRFSTLVSTSR TMR LCC LGLCKPKIVHSNWN- 43
Pan       ILTTLKPPGVSVESKMNNKAGSFFWNLRFSTLVSTSR TMR LCC LGLCKPKIVHSNWN- 43
Pongo    ILTTLKPPGVSVESKMNNKAGSFFWNLRFSTLVPTSR TMR L YRLGLCKPKIVHSNWN- 43
Bos      LXGIRKISRVAQFAGKMTNRAGSFLWNLRLSTLVPTGR TVRLYPLAFCRPN IAYSNWNR 44
Mus      LTYKRIRNTSPDAPLEMNSKARSLLTWIRRFSTLLP RSRALRIDPLGTCRPEVIHSKWNP 44
Gallus   YVLSPLGPFPMVGFPPQIMGYLLNAVRY-LRRCSPVPRPSAPTSRHVVVWTRHRDCLDNTNC 43
          * : : : * : : : : : : : : : *

```

Figure S3. Comparative Protein Sequence analysis of FASTKD2
Panel A. Interspecies alignment of full-length FASTKD2 protein sequences, obtained by ClustalW software online.
 Accession numbers: *Pongo pygmaeus*: ENSPPYG00000013112; *Bos Taurus*: NP_001095587; *Mus musculus*: NP_766010; *Gallus gallus*: XP_421951; *Pan troglodytes*: ENSPTRG00000012848.
Panel B. Predicted sequences corresponding to the translatable ORF of human FASTKD2 protein sequence from the first predicted methionine (M1) to the second methionine (M17). The M1 is consistently absent in non-human species, suggesting that the M1-M17 sequence is not translated and therefore that in humans as in other species the FASTKD2 protein starts from the second potential ATG initiation codon (M17).

Acknowledgments

This work was supported by the Pierfranco and Luisa Mariani Foundation, Fondazione Telethon-Italy grant number GGP07019, the Italian Ministry of University and Research (FIRB 2003 - project RBLA038RMA), the Italian Ministry of Health RF2006 ex 56/05/21, Marie Curie intra-European fellowship (FP6-2005-Mobility-5) number 040140-MAD, and MITOCIRCLE and EUMITOCOMBAT (LSHM-CT-2004-503116) network grants from the European Union framework program 6.

References

1. Zeviani M., Di Donato S. Mitochondrial disorders. *Brain*. 2004;127:2153-2172.
2. Rötig A., Lebon S., Zinovieva E., Mollet J., Sarzi E., Bonnefont J.P., Munnich A. Molecular diagnostics of mitochondrial disorders. *Biochim. Biophys. Acta*. 2004;1659:129-135.
3. Zeviani M. The expanding spectrum of nuclear gene mutations in mitochondrial disorders. *Semin. Cell Dev. Biol.* 2001;12:407-416.
4. Spinazzola A., Zeviani M. Disorders of nuclear-mitochondrial intergenomic communication. *Biosci. Rep.* 2007;27:39-51.
5. Zeviani M., Carelli V. Mitochondrial disorders. *Curr. Opin. Neurol.* 2007;20:564-571.
6. Calvo S., Jain M., Xie X., Sheth S.A., Chang B., Goldberger O.A., Spinazzola A., Zeviani M., Carr S.A., Mootha V.K. Systematic identification of human mitochondrial disease genes through integrative genomics. *Nat. Genet.* 2006;38:576-582.
7. Pagliarini D.J., Calvo S.E., Chang B., Sheth S.A., Vafai S.B., Ong S.E., Walford G.A., Sugiana C., Boneh A., Chen W.K. A mitochondrial protein compendium elucidates complex I disease biology. *Cell*. 2008;134:112-123.
8. Spinazzola A., Viscomi C., Fernandez-Vizarra E., Carrara F., D'Adamo P., Calvo S., Marsano R.M., Donnini C., Weiher H., Strisciuglio P. MPV17 encodes an inner mitochondrial membrane protein and is mutated in infantile hepatic mitochondrial DNA depletion. *Nat. Genet.* 2006;38:570-575.
9. Coulter-Mackie M.B., Applegarth D.A., Toone J., Gagnier L. A protocol for detection of mitochondrial DNA deletions: Characterization of a novel deletion. *Clin. Biochem.* 1998;31:627-632.
10. Bugiani M., Invernizzi F., Alberio S., Briem E., Lamantea E., Carrara F., Moroni I., Farina L., Spada M., Donati M.A. Clinical and molecular findings in children with complex I deficiency. *Biochim. Biophys. Acta*. 2004;1659:136-147.
11. Sobel E., Sengul H., Weeks D.E. Multipoint estimation of identity-by-descent probabilities at arbitrary positions among marker loci on general pedigrees. *Hum. Hered.* 2001;52:121-131.
12. Petruzzella V., Tiranti V., Fernandez P., Ianna P., Carrozzo R., Zeviani M. Identification and characterization of human cDNAs specific to BCS1, PET112, SCO1, COX15, and COX11, five genes involved in the formation and function of the mitochondrial respiratory chain. *Genomics*. 1998;54:494-504.

13. Li W., Simarro M., Kedersha N., Anderson P. FAST is a survival protein that senses mitochondrial stress and modulates TIA-1-regulated changes in protein expression. *Mol. Cell. Biol.* 2004;24:10718-10732.
14. Neupert W. Protein import into mitochondria. *Annu. Rev. Biochem.* 1997;66:863-917.
15. Fernandez-Vizarra E., Lopez-Perez M.J., Enriquez J.A. Isolation of biogenetically competent mitochondria from mammalian tissues and cultured cells. *Methods.* 2002;26:292-297.
16. Wiedemann N., Frazier A.E., Pfanner N. The protein import machinery of mitochondria. *J. Biol. Chem.* 2004;279:14473-14476.
17. Nijtmans L.G., Henderson N.S., Holt I.J. Blue native electrophoresis to study mitochondrial and other protein complexes. *Methods.* 2002;26:327-334.
18. Zhivotosky B., Orrenius S. Assessment of apoptosis and necrosis by DNA fragmentation and morphological criteria. In: Bonifacino J.S., Dasso M., Hardford J.B., Lippincott-Schwartz J., Yamada K.M., editors. *Current Protocols in Cell Biology.* John Wiley & Sons; New York: 2001. Chapter 18, Unit 18.3.
19. Yang J., Liu X., Bhalla K., Kim C.N., Ibrado A.M., Cai J., Peng T.I., Jones D.P., Wang X. Prevention of apoptosis by Bcl-2: Release of cytochrome c from mitochondria blocked. *Science.* 1997;275:1129-1132.
20. Cai J., Jones D.P. Superoxide in apoptosis. Mitochondrial generation triggered by cytochrome c loss. *J. Biol. Chem.* 1998;273:11401-11404.
21. Pavlakis S.G., Phillips P.C., DiMauro S., De Vivo D.C., Rowland L.P. Mitochondrial myopathy, encephalopathy, lactic acidosis, and strokelike episodes: A distinctive clinical syndrome. *Ann. Neurol.* 1984;16:481-488.
22. Bien C.G., Granata T., Antozzi C., Cross J.H., Dulac O., Kurthen M., Lassmann H., Mantegazza R., Villemure J.G., Spreafico R., Elger C.E. Pathogenesis, diagnosis and treatment of Rasmussen encephalitis: A European consensus statement. *Brain.* 2005;128:454-471.

